Quantum Dots

DOI: 10.1002/anie.201105991

Phase Transitions in Quantum-Dot Langmuir Films**

*Karel Lambert, Yolanda Justo, John Sundar Kamal, and Zeger Hens**

The use of Langmuir films of hydrophobic colloidal nanoparticles (NPs) on water surfaces followed by their deposition on a solid substrate is an increasingly popular way of forming 2D nanoparticle superstructures.[1–3] This is mainly inspired by practical advantages. Langmuir–Blodgett (LB) or Langmuir–Schaefer (LS) deposition, in which the Langmuir film is transferred either vertically (LB) or horizontally (LS) to a substrate, leads to well-defined, large-area NP monolayers with a tunable particle density and is not limited to flat substrates. Especially for colloidal quantum dots (QDs), this is a highly attractive processing method because applications such as light-emitting diodes (LEDs),[4] photodetectors,[5] biosensors,[6] and light-harvesting devices[7] require high-quality QD mono- or multilayers. On the other hand, Langmuir films of amphiphilic molecules exhibit a rich and intriguing phase behavior. Langmuir films of saturated carboxylic acids, for example, show a first-order phase transition between a gaseous and a condensed phase that appears as a plateau in the pressure–area π-A isotherm.[8] Similar observations on colloidal NP Langmuir films are rare. Experiments and simulations involving further compression of a NP monolayer usually resulted in layer buckling,[9] or gave only indirect indications of phase transitions.[10,11] Here, we show that the continued compression of monolayers of a variety of colloidal QDs leads to a sequence of plateaus in the π-A isotherm. Using transmission electron microscopy (TEM) and atomic force microscopy (AFM), we show that these plateaus correspond to the consecutive formation of a QD double and triple layer. Moreover, we argue that these transformations correspond to phase transitions in the Langmuir film that can be rationalized based on thermodynamic considerations.

A typical π-A isotherm of 4.0 nm CdSe QDs (Q-CdSe, standard deviation (σ) of 6.9%) on the air/water interface contains different regions (Figure 1). Regions I and II show the usual transition from monolayer islands into a full monolayer.[3] Around 17 mN m^{-1} the slope of the isotherm decreases, indicating layer collapse (i.e. transfer of particles out of the monolayer). However, further compression only leads to a minor pressure increase, creating a plateau in the isotherm (III). Similar plateaus have been reported in studies of Langmuir layers of amphiphilic molecules[12] and hydrophilic Au nanocrystals (NCs),[10] and indicate a phase transition in the layer. When the surface area of the trough is reduced to half the area of the initial full monolayer (A_1), a second increase of the surface pressure is observed (IV), followed by another plateau (V) and again a pressure increase (VI) starting at about $A_1/3$. With bigger CdSe/CdS core/shell particles (6.4 nm, $\sigma = 5.4\%$), the first plateau occurs at a slightly higher pressure (21 mN m^{-1}) and is not entirely flat. No second plateau was observed with these particles. In both systems, further compression is irreversible once the first plateau is reached (see the Supporting Information).

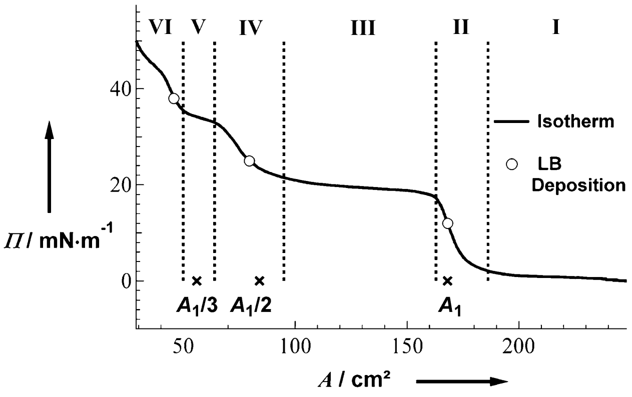

Figure 1. Pressure–area isotherm of a Q-CdSe suspension spread on a water surface, showing different regimes.

Q-CdSe Langmuir films in the steep parts of the isotherm (II, IV, VI) were transferred to silicon substrates using LB deposition. Analysis of such samples reveals microscopic cracks in the multilayer films (see the Supporting Information), which are convenient for film thickness determination using AFM (Figure 2, left side). Height profiles show a stepwise increase in the layer thickness going from region II to IV and VI, indicative of a transition from a monolayer to a bi- and a trilayer. The multilayer roughness is higher than that of the monolayers. It corresponds to monolayer-thick terraces on top of the multilayer, forming longitudinal domains perpendicular to the direction of compression (see the Supporting Information). The cracks are avoided using LS instead of LB deposition, meaning that the cracks are due to the vertical transfer and are not present at the air/water interface. In contrast with CdSe monolayers,[3] CdSe multilayers do not dewet upon LS deposition on hydrophilic substrates. Therefore, LS is favorable over LB deposition of the multilayers. UV/Vis absorbance measurements on layers deposited on glass samples show a linear relationship between the absorbance and the presumed number of layers (see the Supporting Information).

---

[*] K. Lambert, Y. Justo, J. S. Kamal, Prof. Dr. Z. Hens
Physics and Chemistry of Nanostructures, Center for Nano and Biophotonics, Ghent University
Krijgslaan 281–S3, 9000 Gent (Belgium)
E-mail: zeger.hens@ugent.be
Homepage: http://www.nano.ugent.be

[**] Z.H. acknowledges the IWT (SBO Metacel), the FWO-Vlaanderen (grant number G.0144.08), BelSPo (IAP 6.10 photonics@be) and EU-FP7 (ITN Herodot, grant agreement No. 214954) for funding.

Supporting information for this article is available on the WWW under http://dx.doi.org/10.1002/anie.201105991.

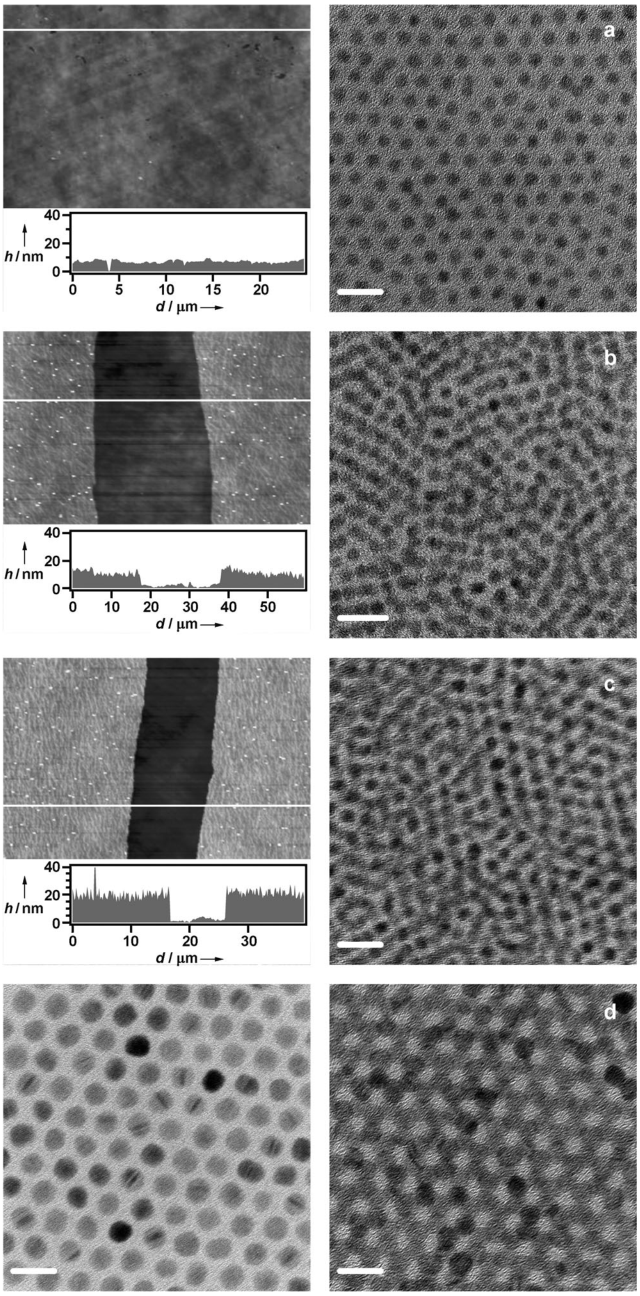

Figure 2. a–c) AFM images, corresponding height (*h*) profiles and TEM images of Langmuir–Blodgett a) monolayer, b) bilayers, and c) trilayers. d) TEM images of Q-CdSe/CdS Langmuir layers deposited at 16 (left) and 39 $\mathrm{mN\,m^{-1}}$ (right). The TEM scale bar corresponds to 10 nm (*d* = distance).

TEM images of CdSe monolayers show a close-packed layer with local hexagonal order (Figure 2a, right side). Layers deposited at 25 $\mathrm{mN\,m^{-1}}$, that is, the second steep rise of the isotherm, show a bilayer, with a more disordered particle stacking (Figure 2b). Compression to 38 $\mathrm{mN\,m^{-1}}$ leads to trilayers with complex structures (Figure 2c). The QD stacking in the bi- and trilayer closely resembles that in multilayers formed by successive Langmuir–Schaeffer deposition.[3] Remarkably, the larger CdSe/CdS core/shell particles form highly ordered monolayers (Figure 2d, left side). The particle stacking in the bilayers is well-defined, as closest-packing occurs (Figure 2d, right side).

Within the plateau regions, lower resolution TEM images show that the Langmuir films consist of a variety of isolated double (Figure 3a) or triple (Figure 3b) layer regions in the first and second isotherm plateau, respectively. These regions can contain a few QDs only (see the Supporting Information) or can extend over several hundreds of nanometers. This strongly indicates that an additional monolayer is formed by locally lifting QDs from the Langmuir film and that these on-top QDs have sufficient mobility to assemble in monolayer islands. Although the overall transition from an n to an $n+1$ layer film ($n \rightarrow n+1$ transition) is not reversible (see the Supporting Information), these observations indicate that the succession of $n \rightarrow n+1$ transitions of the QD Langmuir film can be understood using thermodynamic arguments.

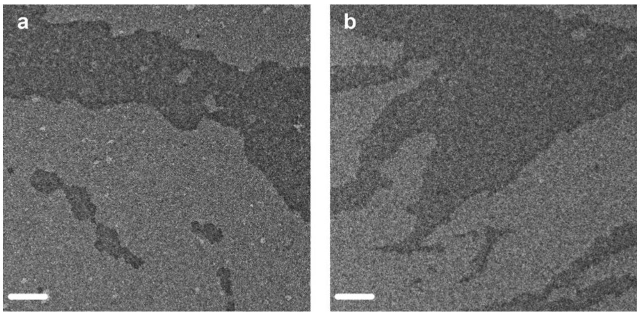

Figure 3. TEM images of Q-CdSe Langmuir films transferred in a) the first isotherm plateau and b) the second isotherm plateau. The scale bar corresponds to 150 nm.

Focusing first on the $1 \rightarrow 2$ transition, this means that this transition becomes possible once the free-energy change of the Langmuir film upon transferring QDs from the monolayer to a bilayer balances the work done in compressing the film [Eq. (1); $n_{\mathrm{QD},1}$ = number of QDs in the monolayer, F = free energy, A = layer area]:

$$\frac{\partial F}{\partial n_{\mathrm{QD},1}} = -\pi \frac{\partial A}{\partial n_{\mathrm{QD},1}} \tag{1}$$

When a QD is transferred from a monolayer to a double layer, the free-energy change involves the loss of lateral QD–QD interactions within the monolayer and the vertical interactions between the QD and the water surface underneath (binding energy u_1), while one gains lateral QD–QD interactions in the second QD layer together with the total vertical interaction energy of a QD in the second layer (binding energy u_2). For the $1 \rightarrow 2$ transition, we can show that the change in lateral QD–QD interaction is a minor contribution (see the Supporting Information). The pressure at which the phase transition occurs is largely given by Equation (2),

$$\pi_{1\rightarrow 2} = \frac{u_2 - u_1}{a_0} \tag{2}$$

where a_0 is the surface area of a single QD in the monolayer.

Equation (2) yields a positive surface pressure when $u_1 < u_2$. Since these are negative numbers (it requires energy to break the interactions), this implies that u_1 must be more negative than u_2, hence the "vertical" interactions must be stronger for a QD in the first layer than for a QD in the second layer. The fact that the QDs initially spread on the water surface in monolayer islands without forming stacks or clusters shows that this is indeed the case. From the experimental π-A isotherms and the area per QD in the Langmuir film, the energy difference $u_2 - u_1$ is calculated as approximately 4 eV. With a projected QD surface area of about 12 nm^2 and a ligand density of 4–5 nm^{-2},[13] about 50 ligands per QD are in touch with the QD/water interface. Hence, the energy differency $u_2 - u_1$ of 4 eV per QD amounts to about 80 meV per ligand or 8 kJ mol^{-1} of ligands, a reasonable value for van der Waals interactions.

If Equation (2) provides an interpretation for the collapse of a QD monolayer, it remains to be demonstrated under which conditions this results in the formation of a double layer. Defining u_3 as the vertical interaction of particles in a trilayer (i.e. with the underlying QD layers and the water surface), an expression similar to Equation (2) can be derived for the bilayer–trilayer transition. As this transition involves the gain of twice u_3 at the expense of u_1 and u_2, we get Equation (3):

$$\pi_{2\to 3} = 2\frac{u_3 - u_2}{a_0} + \frac{u_2 - u_1}{a_0} = 2\frac{u_3 - u_2}{a_0} + \pi_{1\to 2} \qquad (3)$$

We see that $\pi_{2\to 3}$, that is, the pressure where a triple layer is formed, will differ from $\pi_{1\to 2}$ if the u_3 interaction is weaker than the u_2 interaction. Hence, the successive formation of multiple QD layers by compressing a QD Langmuir film requires a gradient in the vertical interactions. The fact that the successive pressure steps are progressively smaller indicates that this gradient disappears with increasing layer number. Hence, we can infer that the energy difference $u_{n+1} - u_n$ tends to zero with increasing n, which limits the number of successive $n \to n+1$ phase transitions.

In summary, we have shown that the compression of QD Langmuir layers beyond their documented collapse pressure results in a successive set of phase transitions into bi- and trilayers. These transitions are displayed by the plateaus in the isotherms. Their occurrence can be rationalized using thermodynamic considerations, which link the pressure required for a phase transition to the difference in vertical interaction energies. The fact that these phase transitions have been observed with CdSe, CdSe/CdS, CdSe/CdS/ZnS, and PbSe QDs (see the Supporting Information) confirms that it is a general behavior of colloidal NP Langmuir films. In the light of the recent results of Murray and co-workers[2] on the formation of binary nanocrystal superlattices at a liquid–air interface, this is an attractive finding that may lead to phase changes in binary superlattices. From a practical perspective, the occurrence of phase transformations in Langmuir films make possible a more efficient use of the LS technique, as the results clearly show that large-scale, high-quality QD multilayers can be transferred to a substrate of choice using a single deposition step. This enhances the potential of the LS technique, for example, to deposit patterned multilayers through microcontact printing.[14]

Experimental Section

Q-CdSe particles are synthesized following Jasieniak et al.[15] Cadmium oxide (CdO, 0.36 mmol, 99.999 %, Strem), oleic acid (OA, 3.6 mmol, 90 %, Aldrich) and *n*-octadecene (ODE, 12 mL, 90 % Alfa Aesar) are mixed and degassed for 1 h at 100 °C in nitrogen, followed by heating to 265 °C until all CdO dissolves. A room-temperature selenium stock solution (16 mL, 0.1M in ODE) is injected. The reaction continues at 235 °C for 16 min. Equal volumes of toluene and isopropanol are added to the crude synthesis mixture, which is then washed four times by precipitation with methanol, and redispersion in toluene.

Q-CdSe/CdS core/shell particles are synthesized using the successive ionic layer adsorption and reaction procedure described by Li et al.[16] Typically, 10^{-5} mmol CdSe cores dispersed in hexane are mixed with 1.5 g *n*-octadecylamine and ODE. After flushing with nitrogen at 100 °C for 1 h, the mixture is heated to 235 °C before injection of the S (0.1M in ODE) and Cd (0.1M in a 10 w % solution of OA in ODE) precursors. The amount of added precursor is calculated to obtain a full monolayer of S or Cd on the particle surface with every injection. The first precursor added is S and the last Cd. The reaction mixture is washed similarly as the CdSe cores after synthesis.

Langmuir layers are produced with a Nima 312D trough. A QD suspension (20–50 μL) is spread dropwise on the water surface (250 cm^2), resulting in a submonolayer which is then compressed at a rate of 10 cm^2 min^{-1}. The layers are transferred on glass or silicon substrates by LS or LB (5 mm min^{-1}) deposition.

TEM samples are prepared by LS deposition on a carbon-coated copper grid and studied with a Jeol 2200 FS microscope. AFM analysis is done with a Molecular Imaging PicoPlus system in AC AFM mode.

Received: August 24, 2011
Published online: October 20, 2011

Keywords: Langmuir–Blodgett films · nanoparticles · phase transitions · quantum dots · self-assembly

---

[1] a) V. Aleksandrovic, D. Creshnykh, I. Randeljelovic, A. Fromsdorf, A. Kornowski, S. V. Roth, C. Klinke, H. Weller, *Acs Nano* **2008**, *2*, 1123; b) A. R. Tao, J. Huang, P. Yang, *Acc. Chem. Res.* **2008**, *41*, 1662.

[2] A. Dong, J. Chen, P. M. Vora, J. M. Kikkawa, C. B. Murray, *Nature* **2010**, *466*, 474.

[3] K. Lambert, R. K. Čapek, M. I. Bodnarchuk, M. V. Kovalenko, D. Van Thourhout, W. Heiss, Z. Hens, *Langmuir* **2010**, *26*, 7732.

[4] P. O. Anikeeva, J. E. Halpert, M. G. Bawendi, V. Bulovic, *Nano Lett.* **2009**, *9*, 2532.

[5] G. Konstantatos, J. Clifford, L. Levina, E. H. Sargent, *Nat. Photonics* **2007**, *1*, 531.

[6] X. Li, Y. Zhou, Z. Zheng, X. Yue, Z. Dai, S. Liu, *Langmuir* **2009**, *25*, 6580.

[7] A. L. Rogach, T. A. Klar, J. M. Lupton, A. Meijerink, J. Feldmann, *J. Mater. Chem.* **2009**, *19*, 1208.

[8] N. R. Pallast, B. A. Pethica, *Langmuir* **1985**, *1*, 509.

[9] a) H. Schwartz, Y. Harel, S. Efrima, *Langmuir* **2001**, *17*, 3884; b) N. I. D. Fenwick, F. Bresme, N. Quirke, *J. Chem. Phys.* **2001**, *114*, 7274; c) L. A. Pugnaloni, R. Ettelaie, E. Dickinson, *Langmuir* **2004**, *20*, 6096; d) D. G. Schultz, X. Lin, D. Li, J. Gebhardt, M. Meron, P. J. Viccaro, B. Lin, *J. Phys. Chem. B* **2006**, *110*, 24522; e) M. K. Bera, M. K. Sanyal, S. Pal, J. Daillant, A.

Datta, G. U. Kulkarni, D. Luzet, O. Konovalov, *Europhys. Lett.* **2007**, *78*, 56003.

[10] M. Fukuto, R. K. Heilmann, P. S. Pershan, *J. Chem. Phys.* **2004**, *120*, 3446.

[11] S. Kubowicz, M. A. Hartmann, J. Daillant, M. K. Sanyal, V. V. Agrawal, C. Blot, O. Konovalov, H. Möhwald, *Langmuir* **2009**, *25*, 952.

[12] C. de Gracia Lux, J. Gallani, G. Watson, M. P. Kraft, *Chem. Eur. J.* **2010**, *16*, 7186.

[13] B. Fritzinger, R. K. Čapek, K. Lambert, J. C. Martins, Z. Hens, *J. Am. Chem. Soc.* **2010**, *132*, 10195.

[14] V. Santhanam, R. P. Andres, *Nano Lett.* **2004**, *4*, 41.

[15] J. Jasieniak, C. Bullen, J. Van Embden, P. Mulvaney, *J. Phys. Chem. B* **2005**, *109*, 20665.

[16] J. J. Li, A. Wang, W. Guo, J. C. Keay, T. D. Mishima, M. B. Johnson, X. Peng, *J. Am. Chem. Soc.* **2003**, *125*, 12567.